Inhibition of *Trypanosoma cruzi* Hexokinase by Bisphosphonates

Michael P. Hudock,[#] C. E. Sanz-Rodríguez,[†] Yongcheng Song,[§] Julian M. W. Chan,[§] Yonghui Zhang,[§] Sarah Odeh,[§] Thomas Kosztowski,[§] Annette Leon-Rossell,[#] J. L. Concepción,[‡] Vanessa Yardley,[⊥] Simon L. Croft,[⊥] Julio A. Urbina,*[,†] and Eric Oldfield*[,#,§]

Department of Biophysics, University of Illinois at Urbana-Champaign, 607 South Mathews Avenue, Urbana, Illinois 61801, Laboratorio de Quimica Biológica, Centro de Biofisica y Bioquímica, Instituto Venezolano de Investigaciones Científicas, Caracas, Venezuela, Department of Chemistry, University of Illinois at Urbana-Champaign, 600 South Mathews Avenue, Urbana, Illinois 61801, Laboratorio de Enzimología de Parásitos, Departamento de Biología, Facultad de Ciencias, Universidad de Los Andes, la Hechicera, Mérida, Venezuela, Department of Infectious and Tropical Diseases, London School of Hygiene and Tropical Medicine, University of London, Keppel Street, London WC1E 7HT, United Kingdom

Received August 18, 2005

Hexokinase is the first enzyme involved in glycolysis in most organisms, including the etiological agents of Chagas disease (*Trypanosoma cruzi*) and African sleeping sickness (*Trypanosoma brucei*). The *T. cruzi* enzyme is unusual since, unlike the human enzyme, it is inhibited by inorganic diphosphate (PPi). Here, we show that non-hydrolyzable analogues of PPi, bisphosphonates, are potent inhibitors of *T. cruzi* hexokinase (TcHK). We determined the activity of 42 bisphosphonates against TcHK, and the IC_{50} values were used to construct pharmacophore and comparative molecular similarity indices analysis (CoMSIA) models for enzyme inhibition. Both models revealed the importance of electrostatic, hydrophobic, and steric interactions, and the IC_{50} values for 17 active compounds were predicted with an average error of 2.4× by using the CoMSIA models. The compound most active against *T. cruzi* hexokinase was found to have a 2.2 μM IC_{50} versus the clinically relevant intracellular amastigote form of *T. cruzi*, but only a ∼1−2 mM IC_{50} versus *Dictyostelium discoideum* and a human cell line, indicating selective activity versus *T. cruzi*.

Introduction

Protozoa are the causative agents of a wide range of diseases including malaria, sleeping sickness, and Chagas disease (caused by *Plasmodium* spp., *Trypanosoma brucei* spp., and *T. cruzi*, respectively[1−3]). In each case, one or more life-cycle stages are dependent on glycolysis for energy production, and consequently, there is interest in the development of specific inhibitors of parasite enzymes involved in glycolysis,[4] including glucose transporters,[5] as novel routes for chemotherapy.

The first enzyme in glycolysis is hexokinase (HK; ATP/hexose-6-phosphotransferase, EC# 2.7.1.1.), which converts glucose into glucose-6-phosphate and in trypanosomatids is localized in a modified peroxisome called the glycosome.[6] In early work, it was found that *T. cruzi* hexokinase (TcHK) was not inhibited by its main regulator in vertebrates, D-glucose-6-phosphate, or by other known vertebrate HK regulators such as fructose-1,6-diphosphate, phosphoenol pyruvate, malate, or citrate, although it was weakly inhibited (competitively with respect to ATP) by ADP.[7,8] More recently however, TcHK was found to be inhibited in a noncompetitive manner (with respect to ATP) by inorganic pyrophosphate (diphosphate, PPi, **1**), with a K_i of ∼500 μM, clearly indicating that PPi acts as an allosteric regulator.[9]

Both trypanosomatid and apicomplexan parasites contain very high levels of PPi [10−12] stored in specialized organelles termed acidocalcisomes,[13] and in earlier work, this observation led us to develop and test a series of hydrolytically stable PPi analogues (called bisphosphonates) as growth inhibitors, with promising results.[10,14,15] We investigated the nitrogen-containing bisphosphonates used to treat bone resorption diseases, pamidronate (**2**), alendronate (**3**), and risedronate (**4**), drugs that are potent inhibitors of the enzyme farnesyl diphosphate synthase (FPPS).[16−23] FPPS catalyses the condensation of isopentenyl diphosphate with dimethylallyl diphosphate to produce, first, geranyl diphosphate, then farnesyl diphosphate, a molecule that is an essential precursor of sterols, dolichols, ubiquinones, and heme *a* and is also directly involved in protein prenylation. We showed that these potent FPPS inhibitors can produce radical cures of both cutaneous[14] and visceral[15] leishmaniasis and also that they have significant activity against *T. cruzi*, both in vitro and in vivo,[10,24,25] and Bouzahzah et al.[26] have reported similar findings in *T. cruzi* with risedronate (**4**) at doses comparable to those used in the treatment of Paget's disease in humans.[27] Interestingly, long alkyl-chain bisphosphonates also inhibit FPPS and *T. cruzi* growth,[28−30] the electrostatic interactions of the basic nitrogen atoms with the protein being replaced, presumably, by van der Waals attractive or dispersion forces in the

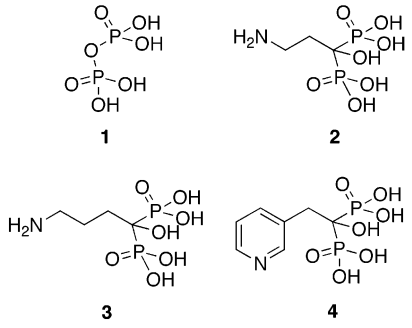

* To whom correspondence should be addressed. For E.O.: Tel (217) 333-3374; fax (217) 244-0997; e-mail eo@chad.scs.uiuc.edu. For J.U.: Instituto Venezolano de Investigaciones Cientificas, Caracas, Venezuela; tel 58-212-504-1660; fax 58-212-504-1093; e-mail jaurbina@cbb.ivic.ve.
[#] Department of Biophysics, University of Illinois at Urbana-Champaign.
[†] Instituto Venezolano de Investigaciones Científicas.
[§] Department of Chemistry, University of Illinois at Urbana-Champaign.
[‡] Universidad de Los Andes.
[⊥] University of London.

10.1021/jm0582625 CCC: $33.50
Published on Web 12/10/2005

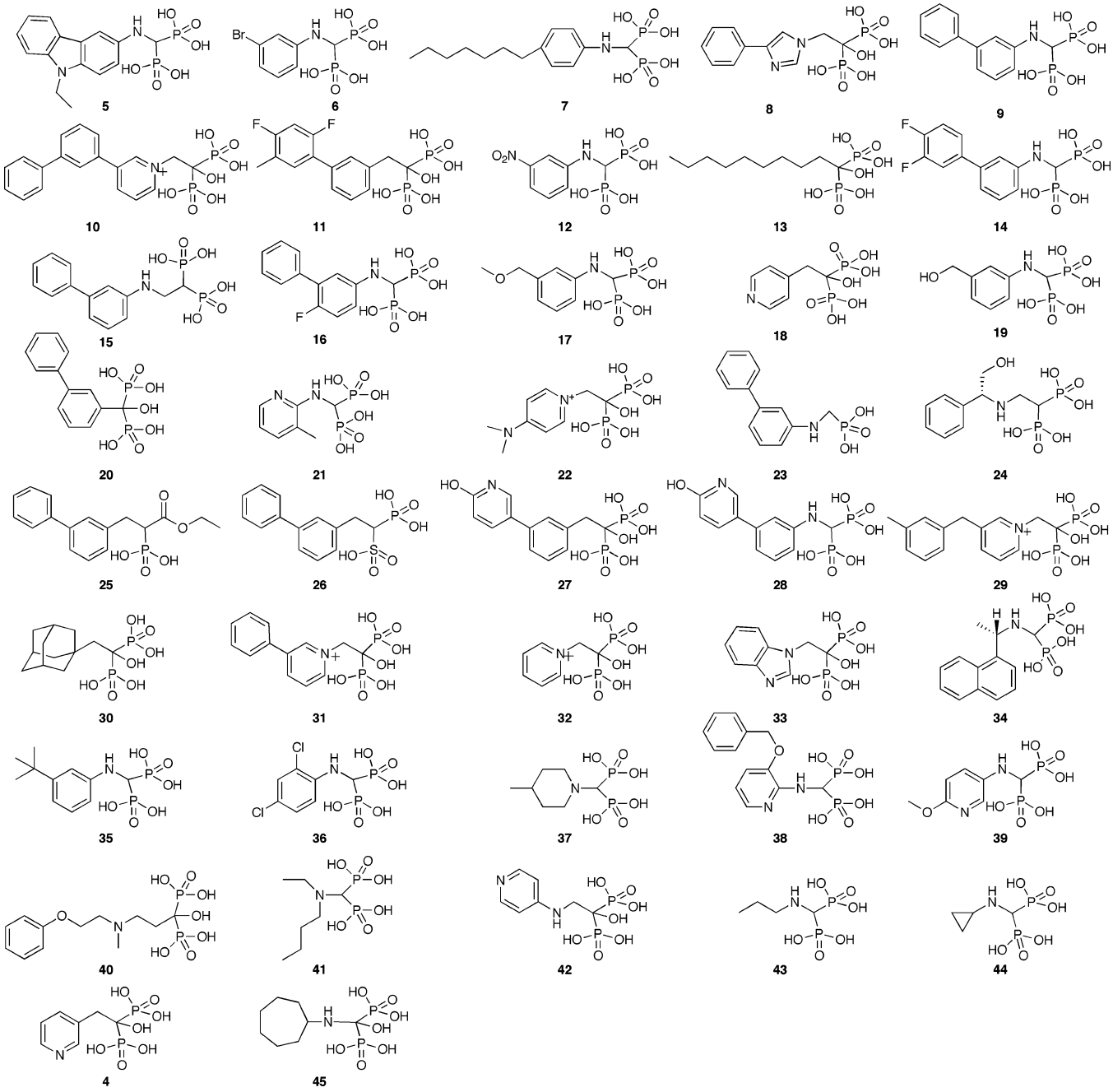

Figure 1. Structures of bisphosphonates investigated in order of decreasing potency in TcHK inhibition.

case of the long alkyl-chain species. Bisphosphonates have also been shown to have activity in inhibiting the resistance of the human AIDS virus, HIV-1, to azidothymidine (AZT).[31] This resistance occurs because mutations in reverse transcriptase permit the phosphorolytic excision of AZT by ATP. Resistance is effectively blocked by some bisphosphonates, which are thought to bind to the excision site in RT since they appear to chemically mimic, to some extent, ATP.[31]

These results indicate that bisphosphonates have utility as antiparasitic agents targeting the FPPS enzyme, but also, they suggested to us that it might be possible to inhibit TcHK by using bisphosphonates that might bind to the PPi allosteric site in TcHK. Here, we describe the discovery of several such bisphosphonates having activity against *T. cruzi* hexokinase, activity in vitro against the clinically relevant intracellular amastigote form of *T. cruzi*, and low cytotoxicity to a human cell line and another eukaryote, *Dictyostelium discoideum* (associated most likely with FPPS inhibition). We use quantitative structure−activity relationship (QSAR) methods to probe the origins of the activities of the bisphosphonates against TcHK (and FPPS), opening up the possibility of developing novel antiparasitic agents targeting, in particular, *T. cruzi* hexokinase.

Materials and Methods

Experimental Section. Synthetic Aspects. The structures of the 42 bisphosphonates investigated, **4**−**45**, are shown in Figure 1. The basic synthetic methods used have been described elsewhere.[32−38] Microchemical analysis results for all new compounds (**8**, **11**, **16**, **22**−**25**, **27**, **28**, **39**, and **42**) were satisfactory and are presented in the Supporting Information (Table S1). All compounds were also routinely characterized by using ^{1}H and ^{31}P NMR spectroscopy at 400 MHz (Varian Unity spectrometer), and representative spectra of the five most active compounds are shown in the Supporting Information. All reagents were purchased from Aldrich. A detailed description of the synthesis of the new compounds follows.

1-Hydroxy-2-(4-phenylimidazol-1-yl)ethylidene-1,1-bisphosphonic Acid (8). Compound **8** was prepared from 4-phenylimidazol-1-ylacetic acid (400 mg, 2 mmol),[39] following general procedure 3 from ref 38 (420 mg, 55% yield). Anal. ($C_{11}H_{13}N_2NaO_7P_2 \cdot H_2O$) C, H, N.

1-Hydroxy-2-[3-(2,4-difluoro-5-methylphenyl)phenyl]ethylidene-1,1-bisphosphonic Acid (11). 3-Methoxycarbonylphenylboronic acid pinacol ester was prepared according to a published procedure[40] starting from methyl 3-bromophenylacetate (0.96 g, 4.2 mmol). The product was then reacted with an equal amount of 5-bromo-2,4-difluorotoluene[41] following general procedure 5 from ref 38, followed by hydrolysis (1 N NaOH), affording 3-(2,4-difluoro-5-methylphenyl)phenylacetic acid as a white powder. Compound **11** was prepared from the acid obtained following general procedure 2 from ref 38 (680 mg, 36% overall yield). Anal. ($C_{15}H_{15}F_2NaO_7P_2 \cdot H_2O$) C, H.

[4-Fluoro-3-phenylphenylamino]methylenebisphosphonic Acid (16). 4-Fluoro-3-phenylaniline was prepared from phenylboronic acid (366 mg, 3 mmol) and *N*-acetyl-3-bromo-4-fluoroaniline (700 mg, 3 mmol) following general procedure 5 from ref 38, followed by acid hydrolysis (3 N HCl, reflux). Compound **16** was made from the aniline obtained following general procedure 1 from ref 38 (400 mg, 35% overall yield). Anal. ($C_{13}H_{14}NFO_6P_2 \cdot H_2O$) C, H, N.

1-Hydroxy-2-(4-dimethylaminopyridinium-1-yl)ethylidene-1,1-bisphosphonic Acid (22). Compound **22** was prepared from 4-(dimethylamino)pyridine (366 mg, 3 mmol) following a published procedure (457 mg, 41% yield).[37] Anal. ($C_9H_{16}N_2O_7P_2 \cdot 0.1$ NaCl) C, H, N.

3-Phenylphenylaminomethylphosphonic Acid (23). A triazine prepared from 3-aminobiphenyl (507 mg, 3 mmol) and formaldehyde (0.25 mL, 37% in H_2O)[42] was heated to 80 °C for 8 h with 2 equiv of diethyl phosphite. The product was purified via column chromatography (silica gel, ethyl acetate) to give the diethyl ester of **23**. Upon treatment with TMSBr as described in general procedure 1 from ref 38, **23** was obtained as a white powder (500 mg, 62% overall yield). Anal. ($C_{13}H_{14}NO_3P \cdot 0.4H_2O$) C, H, N.

2-[(*S*)-1-Phenyl-2-hydroxyethylamino]ethylidene-1,1-bisphosphonic Acid (24). Compound **24** was prepared from (*S*)-1-phenyl-2-hydroxyethylamine (137 mg, 1 mmol) following general procedure 4 from ref 38 (250 mg, 76% yield). Anal. ($C_{10}H_{17}NO_7P_2$) C, H, N.

Ethyl 2-Phosphono-3-(3-phenylphenyl)propionate (25). Triethyl phosphonoacetate (224 mg, 1 mmol) was treated successively with NaH (44 mg, 1.1 mmol, 60% in oil) and 3-bromomethylbiphenyl (247 mg, 1 mmol) in THF, affording the triethyl ester of **25** after column chromatography (silica gel, ethyl acetate). The product was treated with TMSBr as described in general procedure 1 from ref 38 to give **25** as the disodium salt (198 mg, 45% overall yield). Anal. ($C_{17}H_{17}Na_2O_5P \cdot 3.5\ H_2O$) C, H.

1-Hydroxy-2-[3-(6-hydroxypyridin-3-yl)phenyl]ethylidene-1,1-bisphosphonic Acid (27). 3-(6-Methoxypyridin-3-yl)phenylacetic acid was prepared from 6-methoxypyridine-3-boronic acid (306 mg, 2 mmol) and methyl 3-bromophenylacetate (460 mg, 2 mmol) following general procedure 5 from ref 38, followed by hydrolysis (1 N NaOH). Compound **27** was prepared from the acid obtained following general procedure 2 from ref 38, followed by hydrolysis (6 N HCl, reflux) (276 mg, 36% overall yield). Anal. ($C_{13}H_{15}NO_8P_2 \cdot 0.25H_2O$) C, H, N.

[3-(6-Hydroxypyridin-3-yl)phenylamino]methylenebisphosphonic Acid (28). 3-(6-Methoxypyridin-3-yl)aniline was prepared from 6-methoxypyridine-3-boronic acid (306 mg, 2 mmol) and *N*-acetyl-3-bromoaniline (428 mg, 2 mmol) following general procedure 5 from ref 38, followed by acid hydrolysis (3 N HCl, reflux). Compound **28** was made from the aniline obtained following general procedure 1 from ref 38, followed by hydrolysis (6 N HCl, reflux) (400 mg, 35% overall yield). Anal. ($C_{12}H_{14}N_2O_7P_2 \cdot 1.5H_2O$) C, H, N.

(6-Hydroxypyridin-3-yl amino)methylenebisphosphonic Acid (39). Compound **39** was prepared from 3-amino-6-methoxypyridine (372 mg, 3 mmol) following general procedure 1 from ref 38, followed by hydrolysis (6 N HCl, reflux) (270 mg, 32% overall yield). Anal. ($C_6H_{10}N_2O_7P_2$) C, H, N.

2-(Pyridin-4-ylamino)ethylidene-1,1-bisphosphonic Acid (42). Compound **42** was prepared from 4-aminopyridine (94 mg, 1 mmol) following general procedure 4 from ref 38 (150 mg, 49% yield). Anal. ($C_7H_{11}N_2NaO_6P_2$) C, N, H calcd 3.65, found 4.19.

Hexokinase Purification. Native glycosomal TcHK was obtained in a purified form according to Caceres et al.[9]

Enzyme Assays. Hexokinase activity was determined by measuring the production of NADPH at 340 nm using a coupled reaction with D-glucose-6-phosphate dehydrogenase.[8]

Cell Growth Inhibition. *T. cruzi*, *D. discoideum*, and the human KB cell line growth inhibition assays were carried out as described previously.[32,34,37]

Computational Methods. To relate the activity of bisphosphonates to their 3D chemical structures, we used two computational methods, catalyst pharmacophore modeling[43] and comparative molecular similarity indices analysis (CoMSIA).[44] Pharmacophore modeling correlates activity with the presence of chemical features (hydrophobic groups, negative ionizable groups, etc.) and is particularly useful for examining the spatial arrangements of these features, while the CoMSIA method calculates similarity indices based on interactions (e.g., hydrophobic, electrostatic, and steric) between a molecule and a probe and correlates differences in these indices with activity. Both approaches have recently been successfully applied by us to analyze the inhibitory activity of bisphosphonates with for example, an FPPS from *Leishmania major*,[45] a geranylgeranyl pyrophosphate synthase,[46] *Trypanosoma brucei* growth inhibition,[47] and bone resorption.[48]

Pharmacophore modeling was applied to the TcHK activity data using the HipHop and HypoGen modules in Catalyst 4.10.[43] The TcHK inhibition training set included up to 256 conformations of each of the most active compounds within a 20 kcal/mol range from the minimum energy conformer. Two negative ionizable features, two hydrophobic features, and one custom, neutral aromatic ring feature were used to construct the pharmacophores with minimum interfeature spacings of 300 pm, variable weight, and variable tolerance turned on and default values for all other settings. The custom-built neutral aromatic feature was necessary since no default Catalyst feature could account for the variety of ring types present in the compounds investigated.

CoMSIA analyses were performed by using default settings in the Sybyl 7.0 program.[49] Molecular mechanics minimizations using the Tripos force field were carried out in Sybyl 7.0[49] using a convergence criterion requiring a minimum RMS gradient of 0.01 kcal/(mol·Å) at a steepest descent step and an RMS gradient of 0.001 kcal/(mol·Å) at the following Powell[50] and Broyden, Fletcher, Goldfarb, and Shanno (BFGS)[51] steps. Structures were optimized to convergence at each minimization step. Atomic charges for the CoMSIA analyses were determined for the minimized structures by using the Gasteiger−Marsili (GM) method[52] in Sybyl 7.0.[49] In addition, geometry-optimized structures and atomic charges for the most active compounds were calculated using Hartree−Fock theory (the Merz−Singh−Kollman (MK) method[53,54]) in the Gaussian 03 program,[55] employing a 6-31G* basis set. Compounds were aligned to the (H)O−PC−P−O(H) atoms of **5** (Figure 1) using the Align Database command in Sybyl 7.0. CoMSIA indices were calculated on a rectangular grid containing the aligned molecules using hydrophobic, electrostatic, donor, acceptor, and steric fields. The atomic coordinates of the models were then used to compute field values at each point of a 3D grid using the default +1 sp^3 carbon probe and a grid spacing of 2.00 Å. To obtain a quantitative analysis of the dependence of activity on the CoMSIA descriptors, a partial least-squares (PLS) analysis was applied. The optimal number of components for each equation was determined using standard error of prediction values and SAMPLS[56] leave-one-out cross-validation statistics.

Results and Discussion

Recent work from our laboratories has shown that glycosomal hexokinase (HK) from *Trypanosoma cruzi* (TcHK) is inhibited

Table 1. Experimental (IC_{50} and pIC_{50}) and Predicted CoMSIA (pIC_{50}) Results for Bisphosphonate Inhibition of *T. cruzi* Hexokinase, Related Statistics, and Field Contributions

	experimental activity		CoMSIA predicted pIC_{50} (M)											
				test sets [a]										
compd	IC_{50} (μM)	pIC_{50} (M)	training set	1	2	3	4	5	6	7	8	9	pred	error
5	0.81	6.09	6.00	5.87	5.90	5.90	5.88	5.88	5.91	**5.82**	5.97	5.93	**5.82**	0.27
6	0.95	6.02	5.93	5.79	5.70	5.81	5.70	5.70	**5.10**	5.98	5.99	5.92	**5.10**	0.92
7	1.45	5.84	5.96	**5.92**	5.95	5.99	5.81	5.91	5.93	5.94	5.98	5.97	**5.92**	−0.08
8	1.82	5.74	5.67	5.53	**5.12**	5.52	5.52	5.51	5.69	5.66	5.64	5.69	**5.12**	0.62
9	1.95	5.71	5.63	5.72	5.69	**5.64**	5.69	5.69	5.58	5.64	5.70	5.67	**5.64**	0.07
10	2.29	5.64	5.65	5.56	5.50	5.53	5.51	**5.31**	5.72	5.68	5.63	5.73	**5.31**	0.33
11	2.29	5.64	5.57	5.54	5.62	5.53	5.62	5.61	5.58	5.62	5.61	**4.75**	**4.75**	0.89
12	2.40	5.62	5.68	5.78	5.77	5.78	5.74	5.77	5.63	5.65	**5.63**	5.60	**5.63**	−0.12
13	2.75	5.56	5.44	5.19	5.12	5.19	**4.63**	5.14	5.41	5.50	5.43	5.45	**4.63**	0.93
14	2.75	5.56	5.57	5.67	**5.52**	5.61	5.61	5.59	5.54	5.54	5.60	5.61	**5.52**	0.04
15	3.47	5.46	5.55	5.61	5.63	5.61	5.62	5.66	**5.80**	5.47	5.48	5.50	**5.80**	−0.34
16	3.63	5.44	5.54	5.68	5.70	5.63	5.69	5.70	5.53	5.53	**5.62**	5.59	**5.62**	−0.18
17	4.07	5.39	5.33	5.46	5.36	**5.32**	5.34	5.38	5.29	5.33	5.37	5.35	**5.32**	0.07
18	12.60	4.90	4.90	4.94	4.91	4.87	**4.48**	4.86	4.86	4.80	4.94	4.82	**4.48**	0.42
19	14.80	4.83	4.79	**5.29**	4.95	4.96	4.94	4.95	4.89	4.75	4.81	4.77	**5.29**	−0.46
20	34.70	4.46	4.50	4.37	4.38	4.42	4.36	**4.77**	4.58	4.44	4.54	4.46	**4.77**	−0.31
21	45.74	4.34	4.52	4.47	4.40	4.48	4.46	4.39	4.53	**3.63**	4.52	4.27	**3.63**	0.71
30	300	3.52	3.64	3.43	3.45	3.50	3.42	3.47	3.61	3.59	3.64	3.57		
28	300	3.52	3.44	3.63	3.66	3.64	3.69	3.65	3.45	3.47	3.39	3.38		
27	300	3.52	3.58	3.52	3.52	3.47	3.58	3.47	3.52	3.63	3.59	3.50		
25	300	3.52	3.51	3.46	3.45	3.44	3.42	3.39	3.54	3.50	3.48	3.56		
24	300	3.52	3.37	3.37	3.37	3.35	3.36	3.37	3.41	3.50	3.43	3.46		
23	300	3.52	3.48	3.59	3.60	3.60	3.54	3.60	3.49	3.49	3.53	3.56		
22	300	3.52	3.64	3.79	3.77	3.73	3.75	3.84	3.66	3.61	3.68	3.70		
44	300	3.52	3.57	3.61	3.60	3.62	3.58	3.59	3.59	3.54	3.50	3.64		
43	300	3.52	3.42	3.43	3.45	3.45	3.40	3.46	3.35	3.49	3.38	3.46		
4	300	3.52	**4.41**	**4.50**	**4.39**	**4.41**	**4.10**	**4.38**	**4.55**	**4.16**	**4.43**	**4.36**	**4.37**[b]	−0.85
42	300	3.52	**5.28**	**5.42**	**5.36**	**5.36**	**5.03**	**5.23**	**5.14**	**5.10**	**5.30**	**5.27**	**5.25**[b]	−1.73
41	300	3.52	**3.39**	**3.36**	**3.42**	**3.38**	**3.45**	**3.42**	**3.35**	**3.35**	**3.34**	**3.36**	**3.38**[b]	0.14
36	300	3.52	**4.25**	**4.39**	**4.40**	**4.35**	**4.16**	**4.44**	**4.33**	**4.11**	**4.28**	**4.29**	**4.30**[b]	−0.78
38	300	3.52	**4.36**	**4.28**	**4.37**	**4.32**	**4.34**	**4.35**	**4.39**	**4.04**	**4.36**	**4.22**	**4.30**[b]	−0.78
32	300	3.52	**3.37**	**3.37**	**3.42**	**3.37**	**3.34**	**3.36**	**3.42**	**3.09**	**3.34**	**3.28**	**3.34**[b]	0.19
36	300	3.52	**5.27**	**5.29**	**5.24**	**5.28**	**5.18**	**5.22**	**4.95**	**5.23**	**5.30**	**5.35**	**5.23**[b]	−1.71
35	300	3.52	**5.41**	**5.55**	**5.41**	**5.42**	**5.49**	**5.47**	**5.36**	**5.34**	**5.49**	**5.32**	**5.42**[b]	−1.90
34	300	3.52	**3.54**	**3.58**	**3.72**	**3.60**	**3.71**	**3.77**	**3.33**	**3.45**	**3.57**	**3.21**	**3.55**[b]	−0.02
33	300	3.52	**4.47**	**4.57**	**4.46**	**4.48**	**4.12**	**4.43**	**4.76**	**4.24**	**4.48**	**4.47**	**4.45**[b]	−0.92
31	300	3.52	**4.56**	**4.58**	**4.61**	**4.53**	**4.58**	**4.59**	**4.64**	**4.61**	**4.60**	**4.33**	**4.56**[b]	−1.04
45	300	3.52	**3.11**	**3.08**	**3.19**	**3.15**	**3.18**	**3.13**	**3.00**	**3.17**	**3.07**	**3.05**	**3.11**[b]	0.41
29	300	3.52	**3.74**	**3.90**	**3.98**	**3.81**	**3.89**	**4.05**	**3.84**	**3.78**	**3.82**	**3.51**	**3.83**[b]	−0.31
26	300	3.52	**1.59**	**1.64**	**1.82**	**1.73**	**1.87**	**1.83**	**1.90**	**1.71**	**1.48**	**1.55**	**1.71**[b]	1.81
32	300	3.52	**3.95**	**4.00**	**3.97**	**3.94**	**3.85**	**4.00**	**3.88**	**3.97**	**3.98**	**3.88**	**3.94**[b]	−0.42
40	300	3.52	**4.19**	**4.04**	**4.06**	**4.10**	**3.78**	**4.02**	**4.30**	**4.15**	**4.19**	**4.22**	**4.10**[b]	−0.58

		test sets								
	training set	1	2	3	4	5	6	7	8	9
q^2 [c]	0.602	0.55	0.57	0.57	0.62	0.53	0.61	0.61	0.56	0.57
R^2 [d]	0.991	0.98	0.97	0.98	0.98	0.97	0.99	0.99	0.99	0.99
F test [e]	457	207	181	212	249	171	398	638	467	543
N [f]	5	4	4	4	4	4	5	5	5	5
n [g]	24	22	22	22	22	22	22	22	22	22
% electrostatic	42.6	42.7	42.7	41.8	41.4	43.1	43.7	41.9	42.0	44.3
% hydrophobic	24.3	23.5	23.5	24.3	24.5	24.1	23.4	24.5	24.6	23.1
% steric	14.5	14.0	14.0	14.7	14.2	13.5	15.6	14.4	14.0	13.7
% donor	12.0	13.3	13.3	13.0	13.4	12.6	10.8	12.4	12.6	12.0
% acceptor	6.5	6.5	6.5	6.3	6.5	6.7	6.5	6.8	6.7	6.9

[a] Bold values represent predicted activities of compounds that were not included in the training set. Note that test set 9 has only one compound predicted. [b] Average predicted value. [c] Cross-validated R^2. [d] Correlation coefficient. [e] Ratio of R^2 explained to unexplained $= R^2/(1 - R^2)$. [f] Optimal number of principal components. [g] Number of compounds.

by inorganic pyrophosphate,[9] PPi, which acts as a heterotropic allosteric regulator. This observation suggested to us the possibility of designing more potent synthetic PPi analogue molecules, which could also bind into this site, leading to selective TcHK inhibition. We investigate here the activity of a diverse set of such compounds including mono- and bisphosphonates, as well as a phosphonosulfonate, having varied alkyl and 1-, 2-, and 3-ring aryl-containing species, to see to what extent they have activity against TcHK. These compounds were selected from a library of >500 bisphosphonates on the basis of their chemical diversity. Some compounds were indeed found to inhibit TcHK, and the structures of all 42 compounds

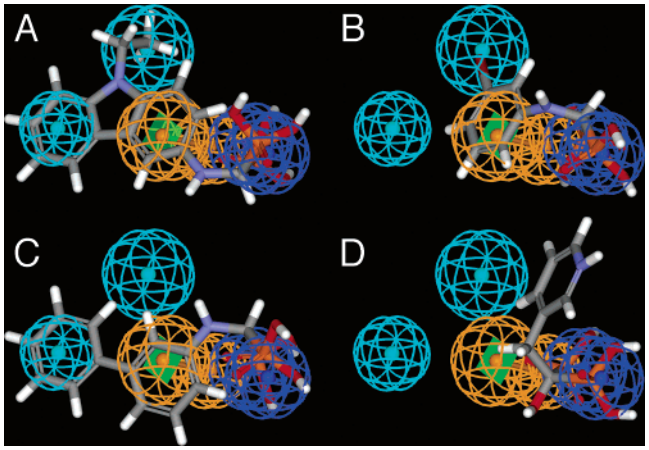

Figure 2. Catalyst pharmacophore for TcHK inhibition superimposed on (A−C) three of the most active compounds, **5**, **6**, and **9**, and (D) risedronate (**4**). The pharmacophore consists of two negative ionizable features (dark blue), two hydrophobic features (cyan), and one neutral aromatic feature (orange).

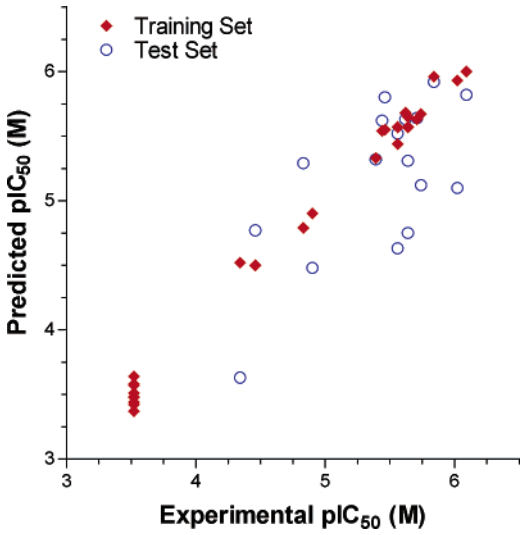

Figure 3. Graphical comparison between experimental and predicted pIC_{50} values for TcHK inhibition: CoMSIA training set (◆) and test set predictions (○). For the training set only, $R^2 = 0.992$; for the test set, $R^2 = 0.44$ with an average 2.4× error in IC_{50} prediction.

investigated are shown in Figure 1, ranked in terms of decreasing potency in TcHK inhibition. The IC_{50} and pIC_{50} (= −log IC_{50} [M]) values for each compound are shown in Table 1. Of the 10 most active compounds (which all have TcHK inhibition activities of <3 μM), it can be seen that eight have relatively large side chains when compared to those present in the bisphosphonates commonly used in bone resorption therapy, such as **2**−**4**. Also of interest is the observation that none of the most potent TcHK bisphosphonates have been reported to have high activity versus an expressed FPPS (from *Leishmania major*, ref 45) or in bone resorption. For example, **5** and **7** have low activity versus FPPS (IC_{50} = 100 μM), and **8** is a very poor inhibitor of bone resorption in rats.[57] On the other hand, several of the compounds that are inactive (IC_{50} = 300 μM) against TcHK are already known to be potent FPPS inhibitors, including species such as risedronate (**4**) and olpadronate (**45**). It thus appears, qualitatively, that activity against TcHK might be associated with the presence of bulky hydrophobic groups and (for the most part) noncharged side chains, while as expected based on previous QSAR investigations,[45,48] FPPS inhibition requires a charged (protonated or pyridinium) side chain, which mimics one or more of the transition state/reactive intermediates that occur in FPP biosynthesis, for the most potent activity. To probe these ideas in more detail, we next investigated the factors that contribute to TcHK inhibition by using the Catalyst pharmacophore modeling approach. We used data for all 17 active species (IC_{50} values of 0.81−46 μM) and the maximum common subgroup method to produce the pharmacophore model shown in Figure 2 superimposed on **5**, **6**, **9**, and **4** (risedronate), Figure 2, panels A−D, respectively. This hypothesis contains, as expected, two negative ionizable groups (the two bisphosphonate groups), in addition to two hydrophobic features and one neutral aromatic ring feature. Two phosphonate groups are clearly required since conversion of **9** into **23** results in loss of all activity seen experimentally. Likewise, the phosphonocarboxylate **25** and the phosphonosulfonate **26** are both inactive (with IC_{50} values of ≥300 μM).

These pharmacophore modeling results are very different from those found previously for bisphosphonates acting as inhibitors of the FPPS enzyme in which the presence of a positive charge feature (mimicking an isoprenoid carbocation transition state/reactive intermediate) plays a key role, and the good correspondence of **4** (risedronate) with the FPPS pharmacophore[45] but poor overlap with the TcHK pharmacophore can be clearly seen in Figure 2D. In fact, our results suggest that HK and FPPS inhibition by bisphosphonates might actually be inversely correlated, that is, good HK inhibitors are generally bad FPPS inhibitors and vice versa. This turns out to be the case for many of the more potent TcHK inhibitors, as discussed below.

Next, we carried out a CoMSIA[44] investigation to see to what extent it might be possible to predict the activities of the compounds shown in Figure 1. This was expected to be difficult given the small range in IC_{50} values and the fact that many compounds investigated had only limits on their activity (i.e., IC_{50} values were ≥300 μM, Table 1). Indeed, in an initial series of calculations using only the 17 active compounds, we found that q^2 values were low, 0.382. We therefore next chose to incorporate a small subset of inactive compounds (**22**, **23**, **24**, **25**, **27**, **28**, **30**, **43**, **44**) into the training set calculations to provide at least some information about which structural features contribute to low potency, then used a reduced training set approach to predict the activities of random groups of active compounds, basically as described previously,[48] to see if predictive utility improved. In addition, these training sets were also used to predict the activity of the "inactives" (IC_{50} ≥ 300 μM). Using this approach, we obtained q^2 values from 0.55 to 0.62 and R^2 values of 0.97−0.99 for the training sets, Table 1, with *F*-test values in the range 171−543. The reduced training set pIC_{50} values for the active test set compounds are shown in bold in the top part of Table 1 and indicate an average pIC_{50} error for the test set predictions of 0.397, corresponding to about a factor of 2.4 error in predicted IC_{50} values. Moreover, 13 of the 16 inactive compounds were correctly identified (predicted activity on average ∼206 μM), showing that this approach has considerable predictive utility. These training and test set results are shown graphically in Figure 3. We also used the data randomization method described previously,[36] assigning random activity values within the range of experimentally determined values to each of the compounds and performing SAMPLS[56] cross-validation. The average q^2 was −0.03 for 100 iterations, considerably lower than the q^2 values obtained using the experimental values in the training and test sets, further validating the CoMSIA results by suggesting that the training and test set results did not occur by chance.

As may be seen in Table 1, the electrostatic field contribution (43%) is large, as is the hydrophobic contribution (24%),

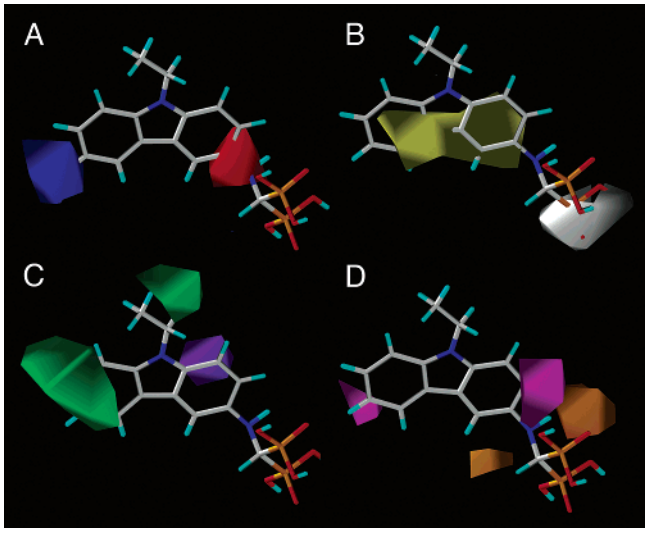

Figure 4. Graphical representation of the CoMSIA fields superimposed on the most active compound, **5**: (A) electrostatic favorable (blue) and unfavorable (red); (B) hydrophobic favorable (yellow) and unfavorable (white); (C) steric favorable (green) and unfavorable (purple); (D) donor favorable (orange) and unfavorable (magenta).

followed by the steric and donor contributions (both ~13−14%). The CoMSIA electrostatic, hydrophobic, steric, and donor fields resulting from the calculations are shown in Figure 4A−D superimposed on the most active compound, **5**, and are clearly similar to the results of the Catalyst pharmacophore modeling study shown in Figure 2. In particular, the positive charge disfavored (red) feature seen in Figure 4A corresponds to the neutral (i.e., not positive) aromatic ring feature (orange) seen in the pharmacophore model, Figure 2. The favored hydrophobic (yellow) and steric (green) field features (Figure 4B,C) correspond to the blue and orange hydrophobic (aromatic ring) features also shown in Figure 2, while the favored donor field (orange) in Figure 4D appears to be associated with the α-NH feature.

These results are of interest since they imply that bisphosphonates, such as the most active TcHK inhibitor, **5**, are unlikely to be toxic to human cells, at least at the level of FPPS inhibition, since they lack the key positive charge feature identified previously in the FPPS (and bone resorption) pharmacophores, and some may be just too large to dock into the FPPS active site. To investigate this topic of selectivity further, we calculated a "therapeutic index" (TI) value defined as

$$\mathrm{TI} = \frac{\mathrm{LD}_{50}(\mathrm{KB})}{\mathrm{IC}_{50}(\mathrm{TcHK})}$$

in which LD_{50} is the concentration of bisphosphonate that kills 50% of a human (nasopharyngeal carcinoma, KB) cell line and IC_{50} is that for TcHK inhibition. This approach enables an estimate of which compounds might be efficacious in human cell-based assays and potentially, in vivo. The numerical results for each compound are given in Table 2. We then plotted these therapeutic indices versus the TcHK IC_{50} values, obtaining the results shown in Figure 5A. Here, the solid circles indicate data points for which discrete LD_{50} values were obtained, while the open circles indicate only lower limits for the therapeutic index, since no toxicity was observed at the highest bisphosphonate levels tested (300 μg mL^{-1}). These results show that TcHK inhibitors such as **5** have relatively low cytotoxicity, and indeed, in a separate assay for cytotoxicity employing *D. discoideum*, Table 2, we found that the majority of the most potent TcHK inhibitors are indeed very poor (millimolar) growth inhibitors against this organism as well.

Table 2. *T. cruzi* Hexokinase IC_{50}, Human Nasopharyngeal Carcinoma (KB) LD_{50}, and *D. discoideum* IC_{50}

compd	TcHK IC_{50} (μM)	KB LD_{50} (μM)	therapeutic index[a]	DD IC_{50} (μM)
5	0.81	698	862	2052
6	0.95	≥771	≥812	112
7	1.44	211	147	10
8	1.81	*b*	*b*	122
9	1.97	827	420	211
10	2.29	*b*	*b*	2
12	2.39	≥635	≥266	78
13	2.77	≥892	≥322	10
14	2.78	≥791	≥285	77
15	3.46	≥560	≥162	62
17	4.06	≥964	≥237	253
18	12.7	1041	82	*b*
19	14.5	≥980	≥67	351
20	35	797	23	103
21	46.2	840	18	3
4	≥300	822	≤2.7	3
45	≥300	163	≤0.5	2
44	≥300	242	≤0.8	30
43	≥300	457	≤1.5	4
42	≥300	384	≤1.3	3
40	≥300	311	≤1.0	2
41	≥300	≥1055	*c*	4
39	≥300	302	≤1.0	52
38	≥300	≥765	*c*	1
37	≥300	446	≤1.5	2
29	≥300	728	≤2.4	889
35	≥300	*b*	*b*	75
34	≥300	*b*	*b*	7
33	≥300	*b*	*b*	2
32	≥300	≥1060	*c*	3
31	≥300	12	≤0.04	3
29	≥300	*b*	*b*	8
22	≥300	*b*	*b*	30

[a] Therapeutic index = KB LD_{50}/TcHK IC_{50}. [b] Value not determined. [c] Indeterminate value.

Of course, it is also necessary that bisphosphonates such as **5** have activity against *T. cruzi* in cell-based assays. To check that activity is in fact seen with the most potent TcHK inhibitors in vitro, we investigated growth inhibition of the intracellular amastigote form of *T. cruzi*. Dose−response curves for **5** and **9** are shown in Figure 5B and yield IC_{50} values of 2.2 μM and 47 μM against this clinically relevant intracellular amastigote form. Since **5** has no significant cytotoxicity to a human cell line (LD_{50} ≥ 0.7 mM) or *D. discoideum* (2.1 mM, Table 2) and has a relatively low IC_{50}, it appears to represent a promising lead for the development of novel specific antiparasitic agents.

It is possible that the lack of toxicity of the most active TcHK inhibitors to the human cell line and to *D.* discoideum is related to the fact that they are expected to be poor inhibitors of FPPS. Of the top 10 TcHK inhibitors, only **8** and **10** have or might be expected to have charged side chains, but apparently, unfavorable steric interactions in the active site of the FPPS enzyme make 2-phenyl-substituted imidazole bisphosphonates poor inhibitors of bone resorption (LED > 3000 μg/kg for 2-phenyl-isozoledronate versus 0.3 μg/kg for isozoledronate[57]), and **10** may be too large to effectively dock into the FPPS active site. On the other hand, small charged species, such as **4**, **40**, and **45,** can all dock into the FPPS active site (there now being a series of crystal structures of **4**−FPPS complexes[58,59]), and all are very active in FPPS inhibition and bone resorption. However these compounds have only one aromatic or hydrophobic feature, not the two or three features identified in the TcHK pharmacophore models. Plus, it appears that the presence of positive charge features found in the potent FPPS inhibitors

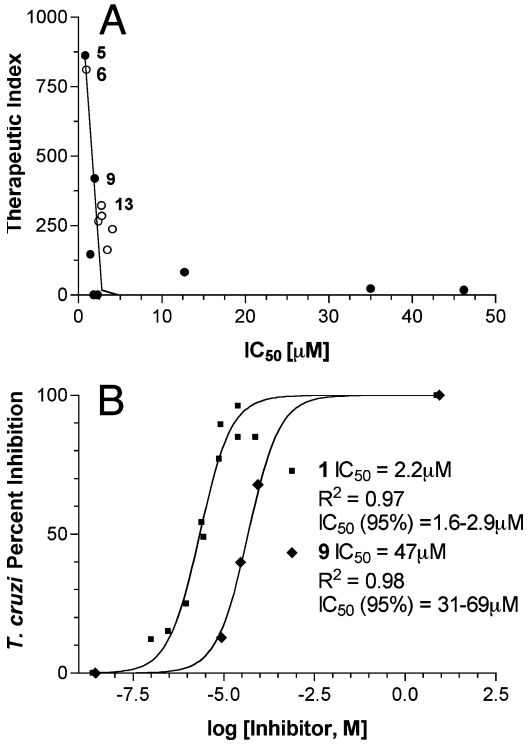

Figure 5. Therapeutic index and *T. cruzi* growth inhibition results; (A) TcHK therapeutic index plot with (●) points where discrete LD_{50} data is available and (○) points where no toxicity was observed at the highest level (300 μg mL^{-1}) tested (a trend line has been added to "guide the eye"); (B) dose−response curve for *T. cruzi* intracellular amastigote growth inhibition for the most active compound, **5**, in addition to **9**. The IC_{50} are 2.2 and 47μM, respectively.

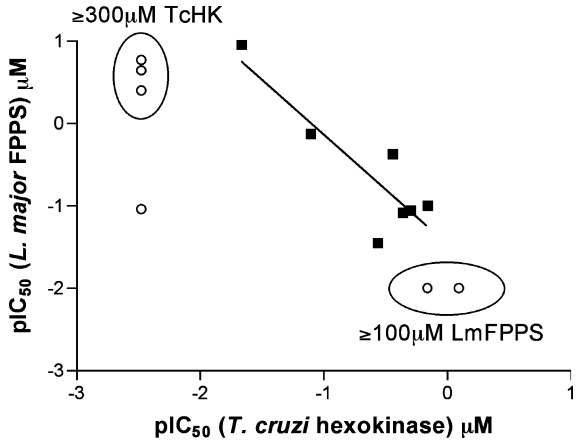

Figure 6. Graph showing proposed inverse correlation between HK and FPPS inhibition by bisphosphonates. Points with discrete values are designated by (■); those with only limit values are designated by (○). The discrete values together with points clustered in the ellipses were used to construct the differential CoMSIA model shown in Figure 7.

decreases TcHK inhibition, opening up the possibility of designing specific TcHK bisphosphonate inhibitors that do not target (human) FPPS. In fact, for many compounds there appears to be an inverse correlation between FPPS inhibition and TcHK inhibition, as shown in Figure 6, where we plot the reported pIC_{50} results for the inhibition of an expressed *Leishmania major* FPPS versus those for TcHK inhibition. The solid squares are for compounds having two discrete IC_{50} values, the open circles indicate that IC_{50} lower limits were observed in one assay.

Since there is a good correlation between the inhibition of *L. major* and human FPPS[23,45] by bisphosphonates, it may be possible in the future to produce TcHK inhibitors that have even less activity against human FPPS and thus less toxicity by using a "difference QSAR" approach based on ΔpIC_{50} data, defined as

$$\Delta pIC50 = pIC_{50}(TcHK) - pIC_{50}(FPPS) = -\log_{10}\left(\frac{IC_{50}(TcHK)}{IC_{50}(FPPS)}\right)$$

in much the same spirit that Khanna et al.[60] have used "sum QSAR" methods to optimize activity against two targets (PPARα and PPARγ), although this approach would naturally be limited to compounds falling close to the correlation line. By way of illustration, we show in Table 3 ΔpIC_{50} values for TcHK/FPPS in which it can be seen that there is a large range in ΔpIC_{50} (~5 units), which encouraged us to determine the CoMSIA fields for selective TcHK inhibition, shown in Figure 7. These results are consistent with those for TcHK and FPPS inhibition alone and emphasize the importance of the increasing steric/hydrophobic features and of reducing positive charge near the bisphosphonate backbone. As more data for human FPPS and TcHK inhibition becomes available, this approach should

Table 3. Differential pIC_{50}[a] Values for *T. cruzi* Hexokinase and *L. major* FPPS Inhibition

	TcHK activity		*L. major* FPPS activity		
compd	IC_{50} (μM)	pIC_{50}	IC_{50} (μM)	pIC_{50}	ΔpIC_{50}[a]
5	0.81	6.09	≥100	4.00	≥2.09
7	1.45	5.84	≥100	4.00	≥1.84
9	1.95	5.71	11.46	4.94	0.77
11	2.29	5.64	12.28	4.91	0.73
13	2.75	5.56	2.37	5.63	−0.07
16	3.63	5.44	28.6	4.54	0.90
18	12.60	4.90	1.34	5.87	−0.97
21	45.74	4.34	0.112	6.95	−2.61
45	≥300	3.52	0.228	6.64	≤−3.12
26	≥300	3.52	11	4.96	≤ −1.44
40	≥300	3.52	0.42	6.38	≤−2.85
4	≥300	3.52	0.17	6.77	≤−3.25

[a] $\Delta pIC_{50} = pIC_{50}(TcHK) - pIC_{50}(FPPS)$.

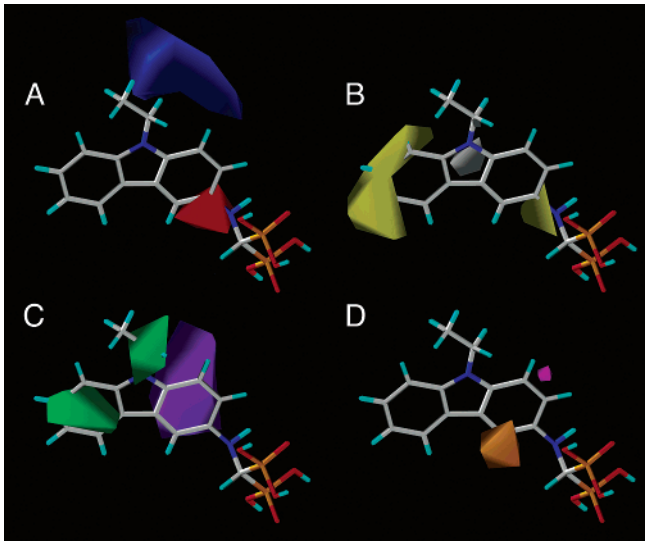

Figure 7. Graphical representation of the differential CoMSIA fields superimposed on the most active compound, **5**: (A) electrostatic favorable (blue) and unfavorable (red); (B) hydrophobic favorable (yellow) and unfavorable (white); (C) steric favorable (green) and unfavorable (purple); (D) donor favorable (orange) and unfavorable (magenta). For this limited data set, the q^2 value was 0.714.

greatly facilitate the development of more potent and selective *T. cruzi* growth inhibitors.

Conclusions

The results that we have discussed above are of interest for several reasons. First, we have found a series of inhibitors of *T. cruzi* hexokinase, some of which are effective against the native enzyme at submicromolar levels. The most potent species is also active against the clinically relevant intracellular amastigote form of *T. cruzi* with an IC_{50} value of 2.2 μM. The most potent TcHK inhibitors are relatively inactive against FPPS, while potent FPPS inhibitors, such as risedronate and incadronate, are inactive versus TcHK. Computational SAR methods provide an explanation of the activity patterns seen in TcHK inhibition and identify the importance of two negative ionizable, one neutral (not positively charged) aromatic, and two hydrophobic pharmacophore features. CoMSIA methods reveal similar features and enable the prediction of the activities of 17 compounds within a factor of 2.4 and correctly select 13/16 inactives (experimental $IC_{50} \geq 300$ μM). The compounds most active against TcHK have little activity against a human cell line or against another eukoryote, *D. discoideum* (IC_{50} values in the 0.5−2 mM range), making *T. cruzi* hexokinase inhibition by bisphosphonates of interest in the development of new chemotherapeutic agents for Chagas disease.

Acknowledgment. This work was supported by the United States Public Health Service (Grant GM-65307 to E.O.); Y.S. was supported by a Leukemia and Lymphoma Society Special Fellowship; J.M.W.C. was supported in part by a Jean Dreyfus Boissevain Fellowship; A.L.-R. was supported by an NIH Training grant (No. GM-08276); J.U. was supported by the Howard Hughes Medical Institute (Grant 55000620); V.Y. and S.L.C. were supported by the World Health Organization Special Programme for Research and Training in Tropical Diseases. We thank J.M. Sanders for valuable suggestions.

Supporting Information Available: Microchemical analysis results for all new compounds (**8**, **11**, **16**, **22**−**25**, **27**, **28**, **39**, and **42**) and ^{1}H and ^{31}P NMR spectra for compounds **8**, **11**, **16**, **22**, and **23**. This material is available free of charge via the Internet at http://pubs.acs.org.

References

(1) *Malaria: Parasite Biology, Pathogenesis, and Protection*; Sherman, I. W., Ed.; ASM Press: Washington, DC, 1998.
(2) Kioy, D.; Jannin, J.; Mattock, N. Human African trypanosomiasis. *Nat. Rev. Microbiol.* **2004**, *2*, 186−187.
(3) Lockman, J. W.; Hamilton, A. D. Recent developments in the identification of chemotherapeutics for Chagas disease. *Curr. Med. Chem.* **2005**, *12*, 945−959.
(4) Lakhdar-Ghazal, F.; Blonski, C.; Willson, M.; Michels, P., Perie, J. Glycolysis and proteases as targets for the design of new antitrypanosome drugs. *Curr. Top. Med. Chem.* **2002**, *2*, 439−456.
(5) Joet, T.; Eckstein-Ludwig, U.; Morin, C.; Krishna, S. Validation of the hexose transporter of *Plasmodium* falciparum as a novel drug target. *Proc. Natl. Acad. Sci. U.S.A.* **2003**, *100*, 7476−7479.
(6) Opperdoes, F. R.; Borst, P. Localization of nine glycolytic enzymes in a microbody-like organelle in *Trypanosoma brucei*: the glycosome. *FEBS Lett.* **1977**, *80*, 360−364.
(7) Urbina, J. A.; Crespo, A. Regulation of energy metabolism in *Trypanosoma (Schizotrypanum) cruzi* epimastigotes. I. Hexokinase and phosphofructokinase. *Mol. Biochem. Parasitol.* **1984**, *11*, 225−239.
(8) Racagni, G. E.; Machado de Domenech, E. E. Characterization of *Trypanosoma cruzi* hexokinase. *Mol. Biochem. Parasitol.* **1983**, *9*, 181−188.
(9) Cáceres, A. J.; Portillo, R.; Acosta, H.; Rosales, D.; Quiñones, W.; Avilan, L.; Salazar, L.; Dubourdieu, M.; Michels, P. A. M.; Concepción, J. L. Molecular and biochemical characterization of hexokinase from *Trypanosoma cruzi*. *Mol. Biochem. Parasitol.* **2003**, *126*, 251−262.
(10) Urbina, J. A.; Moreno, B.; Vierkotter, S.; Oldfield, E.; Payares, G.; Sanoja, C.; Bailey, B. N.; Yan, W.; Scott, D. A.; Moreno, S. N.; Docampo, R. *Trypanosoma cruzi* contains major pyrophosphate stores, and its growth in vitro and in vivo is blocked by pyrophosphate analogues. *J. Biol. Chem.* **1999**, *274*, 33609−33615.
(11) Moreno, B.; Urbina, J. A.; Oldfield, E.; Bailey, B. N.; Rodriques, C. O.; Docampo, R. ^{31}P NMR spectroscopy of *Trypanosoma brucei*, *Trypanosoma cruzi*, and *Leishmania major*. Evidence for high levels of condensed inorganic phosphates. *J. Biol. Chem.* **2000**, *275*, 28356.
(12) Moreno, B.; Bailey, B. N.; Luo, S.; Martin, M. B.; Kuhlenschmidt, M.; Moreno, S. N.; Docampo, R.; Oldfield, E. ^{31}P NMR of apicomplexans and the effects of risedronate on *Cryptosporidium parvum* growth. *Biochem. Biophys. Res. Commun.* **2001**, *284*, 632−637.
(13) Docampo; R.; de Souza, W.; Mirando, K.; Rohloff, P.; Moreno, S. N. J. Acidocalcisomes − conserved from bacteria to man. *Nat. Rev. Microbiol.* **2005**, *3*, 251−261.
(14) Rodriguez, N.; Bailey, B. N.; Martin, M. B.; Oldfield, E.; Urbina, J. A.; Docampo, R. Radical cure of experimental cutaneous leishmaniasis by the bisphosphonate pamidronate. *J. Infect. Dis.* **2002**, *186*, 138−140.
(15) Yardley, V.; Khan, A. A.; Martin, M. B.; Slifer, T. R.; Araujo, F. G.; Moreno, S. N.; Docampo, R.; Croft, S. L.; Oldfield, E. In vivo activities of farnesyl pyrophosphate synthase inhibitors against *Leishmania* donovani and *Toxoplasma gondii*. *Antimicrob. Agents Chemother.* **2002**, *46*, 929−931.
(16) van Beek, E.; Pieterman, E.; Cohen, L.; Lowik, C.; Papapoulos, S. Farnesyl pyrophosphate synthase is the molecular target of nitrogen-containing bisphosphonates. *Biochem. Biophys. Res. Commun.* **1999**, *264*, 108−111.
(17) Cromartie, T. H.; Fisher, K. J.; Grossman, J. N. The discovery of a novel site of action for herbicidal bisphosphonates. *Pestic. Biochem. Physiol.* **1999**, *63*, 114−126.
(18) Keller, R. K.; Fliesler, S. J. Mechanism of aminobisphosphonate action: characterization of alendronate inhibition of the isoprenoid pathway. *Biochem. Biophys. Res. Commun.* **1999**, *266*, 560−563.
(19) Bergstrom, J. D.; Bostedor, R. G.; Masarachia, P. J.; Reszka, A. A.; Rodan, G. Alendronate is a specific, nanomolar inhibitor of farnesyl diphosphate synthase. *Arch. Biochem. Biophys.* **2000**, *373*, 231−241.
(20) Grove, J. E.; Brown, R. J.; Watts, D. J. The intracellular target for the antiresorptive aminobisphosphonate drugs in *Dictyostelium discoideum* is the enzyme farnesyl diphosphate synthase. *J. Bone Miner. Res.* **2000**, *15*, 971−981.
(21) Montalvetti, A.; Bailey, B. N.; Martin, M. B.; Severin, G. W.; Oldfield, E.; Docampo, R. Bisphosphonates are potent inhibitors of *Trypanosoma cruzi* farnesyl pyrophosphate synthase. *J. Biol. Chem.* **2001**, *276*, 33930−33937.
(22) Montalvetti, A.; Fernandez, A.; Sanders, J. M.; Ghosh, S.; Van Brussel, E.; Oldfield, E.; Docampo, R. Farnesyl pyrophosphate synthase is an essential enzyme in *Trypanosoma brucei*. In vitro RNA interference and in vivo inhibition studies.
(23) Dunford, J. E.; Thompson, K.; Coxon, F. P.; Luckman, S. P.; Hahn, F. M.; Poulter, C. D.; Ebetino, F. H.; Rogers, M. J. Structure−activity relationships for inhibition of farnesyl diphosphate synthase in vitro and inhibition of bone resorption in vivo by nitrogen-containing bisphosphonates. *J. Pharmacol. Exp. Ther.* **2001**, *296*, 235−242.
(24) Garzoni, L. R.; Waghabi, M. C.; Baptista, M. M.; de Castro, S. L.; Meirelles, M de N.; Britto, C. C.; Docampo, R.; Oldfield, E.; Urbina, J. A. Antiparasitic activity of risedronate in a murine model of acute Chagas' disease. *Int. J. Antimicrob. Agents* **2004**, *23*, 286−290.
(25) Garzoni, L. R.; Caldera, A.; Meirelles, M de N.; de Castro, S. L.; Docampo, R.; Meints, G. A.; Oldfield, E.; Urbina, J. A. Selective in vitro effects of the farnesyl pyrophosphate synthase inhibitor risedronate on *Trypanosoma cruzi*. *Int. J. Antimicrob. Agents* **2004**, *23*, 273−285.
(26) Bouzahzah, B.; Jelicks, L. A.; Morris, S. A.; Weiss, L. M.; Tanowitz, H. B. Risedronate in the treatment of Murine Chagas' disease. *Parasitol. Res.* **2005**, *96*, 184−187.
(27) Drugs@FDA. http://www.accessdata.fda.gov (date accessed July 2005).
(28) Szajnman, S. H.; Bailey, B. N.; Docampo, R.; Rodriguez, J. B. Bisphosphonates derived from fatty acids are potent growth inhibitors of *Trypanosoma cruzi*. *Bioorg. Med. Chem. Lett.* **2001**, *11*, 789−792.
(29) Szajnman, S. H.; Montalvetti, A.; Wang, Y.; Docampo, R.; Rodriguez, J. B. Bisphosphonates derived from fatty acids are potent inhibitors of *Trypanosoma cruzi* farnesyl pyrophosphate synthase. *Bioorg. Med. Chem. Lett.* **2003**, *13*, 3231−3235.

(30) Szajnman, S. H.; Ravaschino, E. L.; Docampo, R.; Rodriguez, J. B. Synthesis and biological evaluation of 1-amino-1,1-bisphosphonates derived from fatty acids against *Trypanosoma cruzi* targeting farnesyl pyrophosphate synthase. *Bioorg. Med. Chem. Lett.* **2005**, *15*, 4685−4690.
(31) Parniak, M. A.; McBurney, S.; Oldfield, E.; Koontz, D.; Mellors, J. W. Inhibitors of NRTI excision. Presented at the Fourth HIV DRP Symposium, Antiviral Drug Resistance, Dec. 2003, Chantilly, VA; Abstract 29.
(32) Martin, M. B.; Grimley, J. S.; Lewis, J. C.; Heath, H. T., III; Bailey, B. N.; Kendrick, H.; Yardley, V.; Caldera, A.; Lira, R.; Urbina, J. A.; Moreno, S. N. J.; Docampo, R.; Croft, S. L.; Oldfield, E. Bisphosphonates inhibit the growth of *Trypanosoma brucei*, *Trypanosoma cruzi*, *Leishmania donovani*, *Toxoplasma gondii* and *Plasmodium falciparum*: A potential route to chemotherapy. *J. Med. Chem.* **2001**, *44*, 909−916.
(33) Martin, M. B.; Sanders, J. M.; Kendrick, H.; de Luca-Fradley, K.; Lewis, J. C.; Grimley, J. S.; van Brussel, E. M.; Olsen, J. R.; Meints, G. A.; Burzynska, A.; Kafarski, P.; Croft, S. L.; Oldfield, E. Activity of bisphosphonates against *Trypanosoma brucei rhodesiense*. *J. Med. Chem.* **2002**, *45*, 2904−2914.
(34) Ghosh, S.; Chan, J.; Lea, C. R.; Meints, G. A.; Lewis, J. C.; Tovian, Z.; Flessner, R.; Loftus, T. C.; Bruchhaus, I.; de Luca Fradley, K.; Kendrick, H.; Croft, S.; Kemp, R.; Kobayashi, S.; Nozaki, T.; Oldfield, E. Effects of bisphosphonates on the growth of Entamoeba and Plasmodium species in vitro and in vivo. *J. Med. Chem*. **2004**, *47*, 175−187.
(35) Sanders, J. M.; Gomez, A. O.; Mao, J.; Meints, G. A.; Van Brussel, E. M.; Burzynska, A.; Kafarski, P.; Gonzalez-Pacanowska, D.; Oldfield, E. 3-D QSAR investigations of the inhibition of *Leishmania major* farnesyl pyrophosphate synthase by bisphosphonates. *J. Med. Chem.* **2003**, *46*, 5171−5183.
(36) Sanders, J. M.; Ghosh, S.; Chan, J. M.; Meints, G.; Wang, H.; Raker, A. M.; Song, Y.; Colantino, A.; Burzynska, A.; Kafarski, P.; Morita, C. T.; Oldfield, E. Quantitative structure−activity relationships for $\gamma\delta$ T cell activation by bisphosphonates. *J. Med. Chem.* **2004**, *47*, 375−384.
(37) Sanders, J. M.; Song, Y.; Chan, J. M. W.; Zhang, Y.; Jennings, S.; Kosztowski, T.; Odeh, S.; Flessner, R.; Schwerdtfeger, C.; Kotsikorou, E.; Meints, G. A.; Gómez, A. O.; González-Pacanowska, D.; Raker, A. M.; Wang, H.; Morita, C. T.; Oldfield, E. Pyridium-1-yl bisphosphonates are potent inhibitors of farnesyl diphosphate synthase and bone resorption. *J. Med. Chem*. **2005**, *48*, 2957−2963.
(38) Kotsikorou, E.; Song, Y.; Chan, J. M. W.; Faelens, S.; Tovian, Z.; Broderick, E.; Bakalara, N.; Docampo, R.; Oldfield, E. Bisphosphonate inhibition of the exopolyphosphatase activity of the *Trypanosoma* brucei soluble vacuolar pyrophosphatase. *J. Med. Chem.*, in press.
(39) Gil, M. S.; Cruz, F.; Cerdan, S.; Ballesteros, P. Imidazol-1-ylalkanoate esters and their corresponding acids. A novel series of extrinsic proton NMR probes for intracellular pH. *Bioorg. Med. Chem. Lett.* **1992**, *2*, 1717−1722.
(40) Ishiyama, T.; Murata, M.; Miyaura, N. Palladium(0)-catalyzed cross-coupling reaction of alkoxydiboron with haloarenes: a direct procedure for arylboronic esters. *J. Org. Chem.* **1995**, *60*, 7508−7510.
(41) Schweitzer, B. A.; Kool, E. T. Aromatic nonpolar nucleosides as hydrophobic isosteres of pyrimidines and purine nucleosides. *J. Org. Chem.* **1994**, *59*, 7238−7242.
(42) Bouchemma, A,; McCabe, P. H.; Sim, G. A. Conformations of 1,3,5-triaryl-1,3,5-triazacyclohexanes: comparison of the *o*-, *m*-, and *p*-fluorophenyl compounds. *J. Chem. Soc., Perkin Trans. 2* **1989**, *6*, 583−587.
(43) *Catalyst 4.10*; Accelrys Inc.: San Diego, CA; http://www.accelrys.com.
(44) Klebe, G.; Abraham, U.; Mietzner, T. Molecular similarity indices in a comparative analysis (CoMSIA) of drug molecules to correlate and predict their biological activity. *J. Med. Chem.* **1994**, *37*, 4130−4146.
(45) Sanders, J. M.; Gómez, A. O.; Mao, J.; Meints, G. A.; van Brussel, E. M.; Burzynska, A.; Kafarski, P.; González-Pacanowska, D.; Oldfield, E. 3-D QSAR investigations of the inhibition of *Leishmania major* farnesyl pyrophosphate synthase by bisphosphonates. *J. Med. Chem.* **2003**, *46*, 5171−5183.
(46) Szabo, C. M.; Matsumura, Y.; Fukura, S.; Martin, M. B.; Sanders, J. M.; Sengupta, S.; Cieslak, J. A.; Loftus, T. C.; Lea, C. R.; Lee, H. J.; Koohang, A.; Coates, R. M.; Sagami, H.; Oldfield, E. Inhibition of geranylgeranyl diphosphate synthase by bisphosphonates and diphosphates: a potential route to new bone antiresorption and antiparasitic agents. *J. Med. Chem.* **2002**, *45*, 2185−2196.
(47) Martin, M. B.; Sanders, J. M.; Kendrick, H.; de Luca-Fradley, K.; Lewis, J. C.; Grimley, J. S.; van Brussel, E. M.; Olsen, J. R.; Meints, G. A.; Burzynska, A.; Kafarski, P.; Croft, S. L.; Oldfield, E. Activity of bisphosphonates against *Trypanosoma brucei rhodesiense*. *J. Med. Chem.* **2002**, *45*, 2904−2914.
(48) Szabo, C. M.; Martin, M. B.; Oldfield, E. An investigation of bone resorption and *Dictyostelium discoideum* growth inhibition by bisphosphonate drugs. *J. Med. Chem.* **2002**, *45*, 2894−2903.
(49) *SYBYL*, version 7.0; Tripos Inc.: St. Louis, MO.
(50) Powell, M. J. D. Restart procedures for the conjugate gradient method. *Math. Programming* **1977**, *12*, 241−254.
(51) Press, W. H. *Numerical recipes in C: the art of scientific computing*; Cambridge University Press: New York, 1988; p 324.
(52) Gasteiger, J.; Marsili, M. Iterative partial equalization of orbital electronegativity: a rapid access to atomic charges. *Tetrahedron* **1980**, *36*, 3219−3328.
(53) Besler, B. H.; Merz, K. M.; Kollman, P. A. Atomic charges derived from semiempirical methods. *J. Comput. Chem.* **1990**, *11*, 431−439.
(54) Singh, U. C.; Kollman, P. A. An approach to computing electrostatic charges for molecules. *J. Comput. Chem.* **1984**, *5*, 129−145.
(55) Frisch, M. J.; Trucks, G. W.; Schlegel, H. B.; Scuseria, G. E.; Robb, M. A.; Cheeseman, J. R.; Montgomery, J. A., Jr.; Vreven, T.; Kudin, K. N.; Burant, J. C.; Millam, J. M.; Iyengar, S. S.; Tomasi, J.; Barone, V.; Mennucci, B.; Cossi, M.; Scalmani, G.; Rega, N.; Petersson, G. A.; Nakatsuji, H.; Hada, M.; Ehara, M.; Toyota, K.; Fukuda, R.; Hasegawa, J.; Ishida, M.; Nakajima, T.; Honda, Y.; Kitao, O.; Nakai, H.; Klene, M.; Li, X.; Knox, J. E.; Hratchian, H. P.; Cross, J. B.; Bakken, V.; Adamo, C.; Jaramillo, J.; Gomperts, R.; Stratmann, R. E.; Yazyev, O.; Austin, A. J.; Cammi, R.; Pomelli, C.; Ochterski, J. W.; Ayala, P. Y.; Morokuma, K.; Voth, G. A.; Salvador, P.; Dannenberg, J. J.; Zakrzewski, V. G.; Dapprich, S.; Daniels, A. D.; Strain, M. C.; Farkas, O.; Malick, D. K.; Rabuck, A. D.; Raghavachari, K.; Foresman, J. B.; Ortiz, J. V.; Cui, Q.; Baboul, A. G.; Clifford, S.; Cioslowski, J.; Stefanov, B. B.; Liu, G.; Liashenko, A.; Piskorz, P.; Komaromi, I.; Martin, R. L.; Fox, D. J.; Keith, T.; Al-Laham, M. A.; Peng, C. Y.; Nanayakkara, A.; Challacombe, M.; Gill, P. M. W.; Johnson, B.; Chen, W.; Wong, M. W.; Gonzalez, C.; Pople, J. A. *Gaussian 03*, revision C.02; Gaussian, Inc.: Wallingford, CT, 2004.
(56) Bush, B. L.; Nachbar, R. B. Sample-distance partial least-squares: PLS optimized for many variables, with application to CoMFA. *J. Comput.-Aided Mol. Des.* **1993**, 587−619.
(57) Widler, L.; Jaeggi, K. A.; Glatt, M.; Muller, K.; Bachmann, R.; Bisping, M.; Born, A. R.; Cortesi, R.; Guiglia, G.; Jeker, H.; Klein, R.; Ramseier, U.; Schmid, J.; Schreiber, G.; Seltenmeyer, Y.; Green, J. R. Highly potent geminal bisphosphonates. From pamidronate disodium (Aredia) to zoledronic acid (Zometa). *J. Med. Chem.* **2002**, *45*, 3721−3738.
(58) Hosfield, D. J.; Zhang, Y.; Dougan, D. R.; Broun, A., Tari, L. W., Swanson, R. V.; Finn, J. Structural basis for bisphosphonate-mediated inhibition of isoprenoid biosynthesis *J. Biol. Chem.* **2004**, 8526−8529.
(59) Kavanagh, K. L.; Guo, K.; Oppermann, U. Human farnesyl disphosphate synthase complexed with the clinical inhibitor risedronate. http://www.rcsb.org/pdb/, 2005, PDB File 1YV5.
(60) Khanna, S.; Sobhia, M. E.; Bharatam, P. V. Additivity of molecular fields: CoMFA study on dual activators of PPARα and PPARγ. *J. Med. Chem.* **2005**, *48*, 3015−3025.

JM0582625